Metamorphic evolution of the southwest Yilgarn

by

FJ Korhonen, ER Blereau, DE Kelsey, IOH Fielding and SS Romano

Abstract

Metamorphic rocks record information about their pressure (*P*)–temperature (*T*)–time (*t*) evolution in the mineral assemblages, the chemistry and variation in composition of these minerals, and the microstructural relationships among them. Our ability to interpret the evidence recorded by metamorphic rocks is critical to understanding their history and to constraining terrane evolution models. As part of the Accelerated Geoscience Program, quantitative *P–T* estimates were derived from an extensive sample set across the southwest Yilgarn. Such data provide powerful insight into the thermal structure of the crust over time, which, in concert with the expanded whole-rock geochemistry and new interpreted basement structure and geology datasets provided as part of the Accelerated Geoscience Program, provide an excellent foundation for understanding the tectonic and geodynamic framework in which the southwest Yilgarn evolved. The metamorphic data show that granulite and amphibolite facies conditions dominate the project area and corresponding apparent thermal gradients occur between 65 and 208 °C/kbar. Elevated apparent thermal gradients of Neoarchean regional metamorphism were likely partly facilitated by elevated crustal radiogenic heat production.

Methodology and layer details

As of April 2021, *P–T* constraints have been obtained from 28 samples across the southwest Yilgarn (Fig. 1), comprising 17 metasedimentary lithologies, three felsic gneisses and eight mafic lithologies. Metamorphic estimates were derived using phase equilibria modelling based on bulk rock chemical compositions (Fig. 2). These composition-specific phase diagrams were calculated using the software THERMOCALC version tc340 (Powell and Holland, 1988) and the internally consistent thermodynamic dataset of Holland and Powell (2011; dataset tc-ds62) for metasedimentary and felsic lithologies and Green et al. (2016; dataset tc-ds63) for mafic lithologies. The chemical systems used for the modelling were selected to include the key elemental components of each sample in order to most closely approximate the actual rock composition; however, the model system is a necessary simplification of the more complex natural system. The metasedimentary samples were generally modelled in the MnNCKFMASHTO ($MnO–Na_2O–CaO–K_2O–FeO–MgO–Al_2O_3–SiO_2–H_2O–TiO_2–O$) system, and mafic samples were modelled in the NCKFMASHTO system. The activity–composition relations used in the modelling for metasedimentary and felsic lithologies are detailed in White et al. (2014a,b), and those used for mafic lithologies are detailed in Green et al. (2016). The interpretation of phase diagrams utilizes detailed petrography to identify the peak assemblage and any possible metamorphic reactions preserved in the rock, manifest as overprinting relationships. Mineral chemistry, thermobarometry and in situ monazite geochronology for samples with such data were also used to further constrain the *P–T–t* evolution. Details for each sample, including location, geologic context, petrographic description, methodology, results, and interpretation, are summarized in the corresponding Metamorphic History Record. The results in this layer are considered to be preliminary until the Metamorphic History Record for a sample has been released. Future *P–T* estimates and age results from additional samples not included on the layer will be released on GeoVIEW.WA as they become available. Additional information on the workflow with relevant background and methodology are provided in Korhonen et al. (2020).

The layer captures several attributes that are relevant for understanding the metamorphic evolution of the southwest Yilgarn. These attributes are summarized in the data dictionary for this layer, but key attributes are elaborated on here. Unless otherwise specified, reported metamorphic ages herein are based on in situ monazite geochronology using laser ablation inductively coupled plasma mass spectrometry (LA-ICP-MS), and details are or will be available in the corresponding Geochronology Record on GeoVIEW.WA. The *P*–*T* data for peak metamorphic conditions (M_{pk}) are based on the calculated stability of the peak phase assemblage (Fig. 2). The minimum and maximum values for *P* and *T* are recorded in the data layer, as well as the median value, which are defined by the size of the peak assemblage stability field. An assessment of uncertainty is also provided, which is defined as half of the data range (i.e. the difference between the median and the maximum or minimum values). An uncertainty of '1000' flags a result with only a minimum or maximum constraint, and thus has no data range or median value. For these samples, the minimum or maximum value is reported as the median. The apparent thermal gradient is also calculated for each sample using the minimum, maximum and median *P* and *T* values, defined as the *T/P* ratio, in °C/kbar. The median peak *P*, *T*, and apparent thermal gradient are plotted in three separate digital layers. Warm symbol colours represent higher values, decreasing to cooler colours. Five symbol sizes are used for each layer that correspond to the reliability of the result. Larger symbols represent samples that are more tightly constrained with smaller data ranges and therefore smaller uncertainty. The smallest symbol is for samples with only a minimum or maximum constraint.

Some samples preserve information on the post peak history (M_{rg}), which can be used to infer a retrograde *P*–*T* trajectory following conditions of peak metamorphism. For these samples, M_{rg} conditions are generally interpreted to be the *P*–*T* conditions of melt crystallization. The minimum, maximum and median values for M_{rg} *P*, *T* and apparent thermal gradient are reported for these samples, as well as the uncertainty defined as half of the data range for each parameter.

Many of the samples modelled in this study were collected and analysed as part of the unpublished Yilgarn Craton Metamorphic Project (2003–2014). The results from this project have not been released by the Geological Survey of Western Australia (GSWA), although select data are available in Goscombe et al. (2019) using an alternative sample number that is included in the data layer. The layer captures published *P*–*T* estimates from Goscombe et al. (2019), derived from multiple reaction thermobarometry (avPT in THERMOCALC; Powell and Holland, 1988) and/or conventional thermobarometry. Although these thermobarometric estimates are provided, they have not been integrated with the *P*–*T* estimates constrained by phase equilibria modelling and thus remain standalone. Any additional information regarding the metamorphic estimate or age for the sample are included in the 'COMMENTS' field.

P–T–t results

The quantitative *P*–*T* data from all the samples indicate peak metamorphism under amphibolite to granulite facies conditions, consistent with observations from previous studies (e.g. Gee et al., 1981). However, due to the limited exposure of lithologies that typically grow informative metamorphic minerals and low-variance mineral assemblages which can be used to constrain *P*–*T* conditions, there are data gaps across the project area, particularly in the northeast and southwest (Fig. 1). The majority of samples analysed thus far are from the northwest-trending Corrigin Tectonic Zone (CTZ), with others more proximal to the Youanmi Shear Zone to the east and to the Darling Fault in the west (Fig. 1).

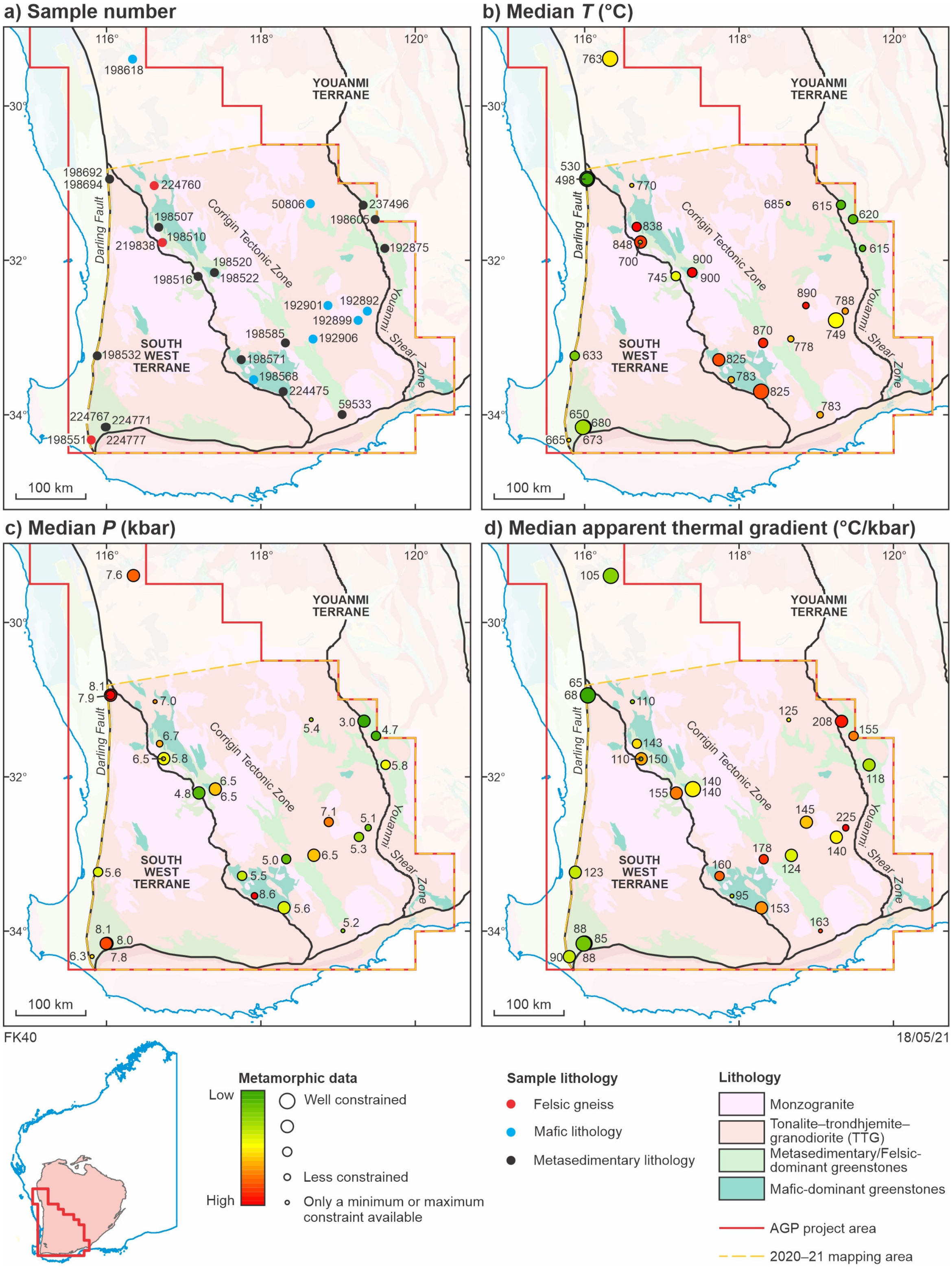

Figure 1. Sample locations and metamorphic data as of April 2021: a) sample location map; b) median *T*; c) median *P*; d) median apparent thermal gradient. Bedrock geology within the 2021–21 mapping area from Quentin de Gromard et al. (2021); other geology based on available 1:500 000 interpreted bedrock geology layers

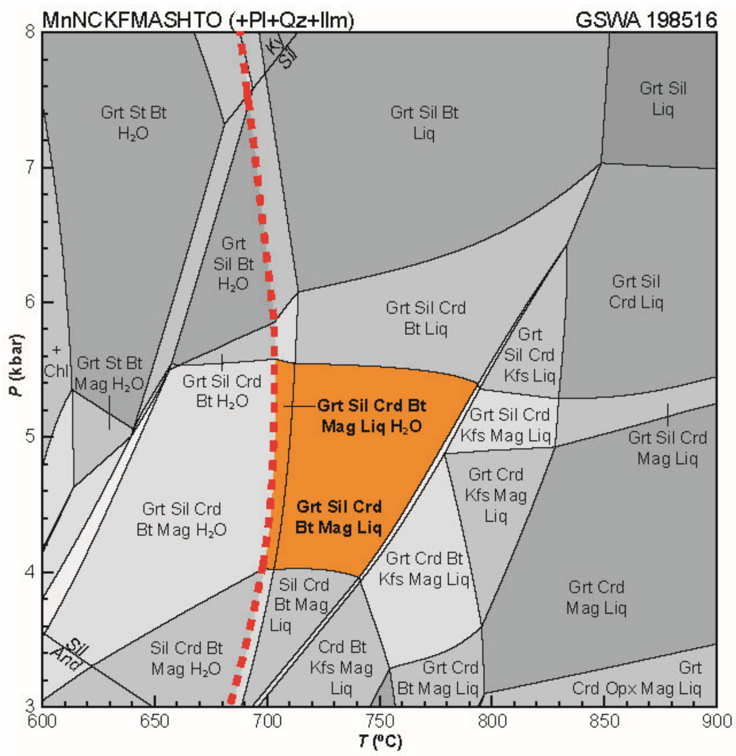

Figure 2. Example of *P–T* phase diagram calculated for a bulk rock chemical composition (GSWA 198516). The *P–T* data for peak metamorphic conditions are based on the calculated stability of the peak phase assemblage, and the minimum and maximum values are defined by the size of the peak assemblage stability field (shown in orange shading with bold text). Red dashed line represents the solidus. Mineral abbreviations provided in Korhonen et al. (2020)

Temperature

High-temperature granulites with median temperatures (T_{med}) between 700 and 900 °C occur within the CTZ (Fig. 1b), a broad zone of ductile transpressional shear zones (Ivanic, 2021; Quentin de Gromard et al., 2021) that forms the redefined boundary (Quentin de Gromard et al., 2021) between the Youanmi and South West Terranes. The timing of high-grade metamorphism and tectonism in this zone is estimated at 2665–2635 Ma, based on U–Pb analyses of monazite from several metamorphic samples (e.g. Fielding et al., 2021a–d) and ages obtained from metamorphic zircon rims (e.g. Wingate et al., 2008; 2021a,b; Lu et al., 2020). The *P–T* estimates for samples that record older ages of c. 2665 Ma (e.g. GSWA 219838) cannot be distinguished from samples that record younger ages of 2655–2635 Ma (e.g. GSWA 198522), supporting a model for a protracted high-*T* event over 30 Ma. This age range extends the timing of high-grade metamorphism previously estimated at 2649–2640 Ma (e.g. Nemchin et al., 1994). To the east of this zone, elevated metamorphic temperatures (>750 °C) are broadly similar to the results from the CTZ (Fig. 1b), although a full interpretation of this data is limited by poor spatial coverage and results with larger *P–T* uncertainties. There are also no metamorphic age constraints available for this part of the project area, as most of the samples are mafic granulites that do not contain datable metamorphic minerals. Distinctly lower temperatures are recorded from samples east of the Youanmi Shear Zone (620–615 °C) and along the western margin near the Darling Fault (680–500 °C; Fig. 1b). The metamorphic samples along the western margin yield a range of Proterozoic ages, with little evidence of the older Archean history preserved. The timing and significance of the Proterozoic reworking is currently being evaluated, although recent mapping within and just east of the Darling Fault supports a polyphase geological history spanning from the Archean to the Mesozoic (Zibra, 2021).

Pressure

Peak pressures (meaning pressures at the peak *T*) across the project area typically range from 4.7 to 6.8 kbar (Fig. 1c), corresponding to mid-crustal depths between about 16 and 24 km by c. 2665 Ma. The majority of the samples in the CTZ record peak pressures of 5.5 – 6.5 kbar, although lower and higher values are also reported. Samples to the east record broadly similar pressures indicating a similar exposed crustal level, although these results are subject to the same data caveats described above. One sample to the east of the Youanmi Shear Zone in the Southern Cross greenstone belt records a distinctly lower *P* of 3.0 kbar (GSWA 237496). Monazite in a metapelitic schist from the same drillcore yields two age components at c. 2670 and 2630 Ma (Fielding et al., 2021e), suggesting a similar age of metamorphism to the CTZ in this part of the project area. Samples along the western margin near the Darling Fault record notably higher pressures, with peak Proterozoic pressures up to 8.1 kbar (Fig. 1c).

Apparent thermal gradients

Classifying *P–T* data in terms of apparent thermal gradients provides a way of normalizing variations in the crustal depth that is exposed, and instead focusing on the thermal regime that existed at the time of metamorphism. The apparent thermal gradients calculated from the peak *P–T* estimates show relatively uniform values across the project area. Within the CTZ and to the east, the most well constrained samples record apparent thermal gradients typically between 120 and 160 °C/kbar (Fig. 1d). These values straddle the upper limit for high *T/P* ('Barrovian') and lower limit of ultrahigh *T/P* (see Korhonen et al., 2020) and are generally higher than the range observed from other Neoarchean metamorphic events compiled by Brown and Johnson (2018; fig. 3). The two samples within the Southern Cross greenstone belt east of the Youanmi Shear Zone have values of 155 and 208 °C/kbar (Fig. 1d), which are broadly similar to the results from Dalstra et al. (1999). These conditions have been attributed to regional contact metamorphism during the emplacement of voluminous high Ca-granites (Dalstra et al., 1999) and synchronous granite doming and regional folding (Doublier et al., 2014).

Much lower thermal gradients are recorded by the Proterozoic samples along the western margin (65–90 °C/kbar; Fig. 1d). These values are within the range expected for high *T/P* ('Barrovian') metamorphism, but indicate significantly cooler conditions in the crust compared to the 2665–2635 Ma metamorphic event. The *P–T* conditions indicate crustal thickening and burial to depths up to about 28 km; however, metamorphic ages along this margin indicate a polyphase history and the timing of burial, peak metamorphism, and any subsequent reworking has not been firmly established or resolved.

Retrograde history

In this dataset, ten samples preserve evidence for post-peak (M_{rg}) conditions, and eight of those samples can be used to infer a retrograde *P–T* path. Of these eight samples, six are from within the CTZ, and two are located east of the Youanmi Shear Zone. Clockwise *P–T* paths were determined from six of the samples, including the two eastern samples, generally supporting a history of burial and heating. Two potential anticlockwise paths were independently retrieved from the same locality in the central CTZ (GSWA 198520, 198522), whereas a potential clockwise path was recorded in a sample located about 20 km to the west in the footwall of the CTZ (GSWA 198516). Monazite from these three samples yield similar peak metamorphic ages from c. 2656 to 2647 Ma. Although these contrasting trajectories might have tectonic significance, the results for all three samples are also compatible with near isobaric cooling paths. The apparent thermal gradients calculated for peak (M_{pk}) and retrograde (M_{rg}) conditions for the 10 samples are very similar, indicating little change to the thermal structure of the crust during cooling from peak conditions to melt crystallization.

Role of radiogenic heat production for Neoarchean metamorphism in the southwest Yilgarn

The crustal evolution of the southwest Yilgarn is characterized by voluminous granite magmatism between 3010 and 2610 Ma. A compilation of all inferred Archean rock types sampled in the southwest Yilgarn shows that the crustal rocks are elevated in radiogenic heat production (Fig. 3) with an average value in the dataset of 7.1 μWm^{-3} (n=1260) at 2640 Ma, compared to the global crustal average of 2.78 μWm^{-3} (calculated at 2640 Ma). The granites typically have the highest concentrations of heat-producing elements (HPE) in the dataset, although granites with higher HPEs have whole rock major element compositions that are broadly similar to granites with lower HPEs

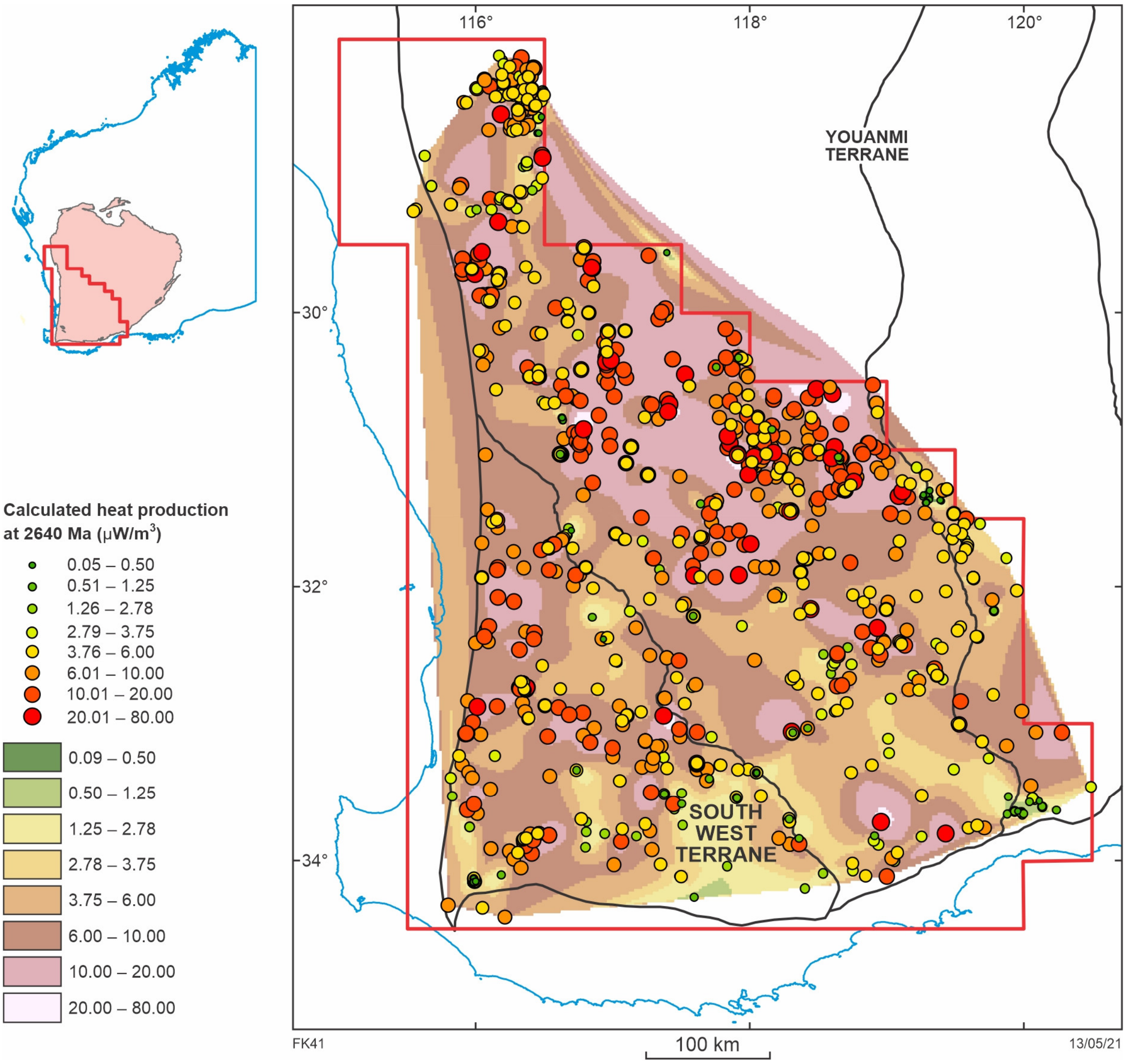

Figure 3. Calculated radiogenic heat production at 2640 Ma for samples of all lithologies within the project area, showing point data and contoured raster image using the Natural Neighbour interpolation tool in ArcGIS Spatial Analyst. The global whole crust average and upper crust average radiogenic heat production at 2640 Ma are 2.78 μWm^{-3} and 3.75 μWm^{-3}, respectively (from Wedepohl, 1995, geochemical data)

(Smithies et al., 2021), indicating that elevated heat production reflects the source characteristics, and is not restricted to low degree partial melts. A long history of elevated heat production in the crust is implied by the calculated heat production of granitic rocks that make up a significant portion of the southwest Yilgarn crust, which were emplaced prior to, synchronous with, and following the 2665–2635 Ma metamorphism. In addition, amphibolite to granulite facies supracrustal rocks in the southwest Yilgarn also have elevated radiogenic heat production values (on average 3.3 μWm^{-3}, n=27; Fig. 3). Together these imply that at the time of 2665–2635 Ma high-*T* metamorphism, and at the depth where amphibolite to granulite facies metamorphism was occurring, the crust was strongly enriched in HPEs, and that magmatism occurring during 2665–2635 Ma metamorphism was sourced from crust with elevated radiogenic heat production. These elevated thermal conditions are also exemplified by a northwest-trending belt of extreme heat production (>10 μWm^{-3}; Fig. 3) in the northern part of the study area that contain low-Ca, high-phosphorus granites with high zircon saturation temperatures (850–950 °C; Smithies et al., 2021), and chemical compositions that are consistent with high-*T* felsic magmatism (Smithies et al., 2021). These results suggest that large regions of the project area reflect zones of unusually high heat flow both in the source and at the level of emplacement. The thermal drivers for these extreme conditions were likely a combination of elevated crustal heat production (Fig. 3), the effects of regional-scale granite magmatism, and a juvenile mantle contribution at depth.

How to access

The Compilation of metamorphic history information data layer is available on a USB via the DMIRS eBookshop.

References

Brown, M and Johnson, T 2018, Secular change in metamorphism and the onset of global plate tectonics: American Mineralogist, v. 103, no. 2, p. 181–196, doi:10.2138/am-2018-6166.

Dalstra, HJ, Ridley, JR, Bloem, EJM and Groves, DI 1999, Metamorphic evolution of the central Southern Cross Province, Yilgarn Craton, Western Australia: Australian Journal of Earth Sciences, v. 46, p. 765–784.

Doublier, MP, Thébaud, N, Wingate, MTD, Romano, SS, Kirkland, CL, Gessner, K, Mole, DR and Evans, N 2014, Structure and timing of Neoarchean gold mineralization in the Southern Cross district (Yilgarn Craton, Western Australia) suggest leading role of late Low-Ca I-type granite intrusions: Journal of Structural Geology, 67, Part B, p. 205–221, doi:10.1016/j.jsg.2014.02.009.

Fielding, IOH, Wingate, MTD, Korhonen, FJ and Rankenburg, K 2021a, 198516: pelitic granofels, Quajabin Peak; Geochronology Record 1764: Geological Survey of Western Australia, in prep.

Fielding, IOH, Wingate, MTD, Korhonen, FJ and Rankenburg, K 2021b, 198520: pelitic granofels, Tregenza Road; Geochronology Record 1765: Geological Survey of Western Australia, in prep.

Fielding, IOH, Wingate, MTD, Korhonen, FJ and Rankenburg, K, 2021c; 198522: pelitic granofels, Tregenza Road; Geochronology Record 1766: Geological Survey of Western Australia, in prep.

Fielding, IOH, Wingate, MTD, Korhonen, FJ and Rankenburg, K 2021d, 219838: granitic gneiss, Mount Mackie; Geochronology Record 1772: Geological Survey of Western Australia, in prep.

Fielding, IOH, Wingate, MTD, Lu, Y, Korhonen, FJ and Rankenburg, K 2021e, 237497: pelitic gneiss, Sunbeam pit; Geochronology Record 1773: Geological Survey of Western Australia, in prep.

Gee, RD, Baxter, JL, Wilde, SA and Williams, IR 1981, Crustal Development in the Archaean Yilgarn Block, Western Australia: Geological Society of Australia, Special Publication 7, 43–56.

Goscombe, B, Foster, DA, Blewett, R, Czarnota, K, Wade, B, Groenewald, B and Gray, D 2019, Neoarchaean metamorphic evolution of the Yilgarn Craton: a record of subduction, accretion, extension and lithospheric delamination: Precambrian Research, article no. 105441, doi:10.1016/j.precamres.2019.105441.

Green, ECR, White, RW, Diener, JFA, Powell, R, Holland, TJB and Palin, RM 2016, Activity–composition relations for the calculation of partial melting equilibria in metabasic rocks: Journal of Metamorphic Geology, v. 34, no. 9, p. 845–869.

Holland, TJB and Powell, R 2011, An improved and extended internally consistent thermodynamic dataset for phases of petrological interest, involving a new equation of state for solids: Journal of Metamorphic Geology, v. 29, no. 3, p. 333–383.

Ivanic, TJ 2021, Dyke and structure density of the southwest Yilgarn: Geological Survey of Western Australia, digital data layer, <https://www.dmirs.wa.gov.au/geoview>.

Korhonen, FJ, Kelsey, DE, Fielding IOH and Romano, SS 2020, The utility of the metamorphic rock record: constraining the pressure–temperature–time conditions of metamorphism: Geological Survey of Western Australia, Record 2020/14, 24p.

Lu, Y, Wingate, MTD and Smithies, RH 2020, 219902: metagranodiorite, Jinkas Hill mine; Geochronology Record 1686: Geological Survey of Western Australia, 5p.

Nemchin, AA, Pidgeon, RT and Wilde, SA 1994, Timing of Late Archaean granulite facies metamorphism in the southwestern Yilgarn Craton of Western Australia: Evidence from U–Pb of zircons from mafic granulites: Precambrian Research, v. 68, no. 3-4, p. 307–321.

Powell, R and Holland, TJB 1988, An internally consistent dataset with uncertainties and correlations: 3. Applications to geobarometry, worked examples and a computer program: Journal of Metamorphic Geology, v. 6, no. 2, p. 173–204.

Quentin de Gromard, R, Ivanic, TJ and Zibra, I 2021, Pre-Mesozoic Interpreted Bedrock Geology of the southwest Yilgarn, 2021: Geological Survey of Western Australia, digital data layer, <https://www.dmirs.wa.gov.au/geoview>.

Smithies, RH, Lu, Y, Lowrey, J, Ivanic, T, Champion, DC and Wilde, SA 2021, Variations in granite geochemistry in the southwest Yilgarn: Geological Survey of Western Australia, digital data layer, <http://www.dmirs.wa.gov.au/geoview>.

Wedepohl, KH 1995 The Composition of the Continental Crust. Geochimica et Cosmochimica Acta, v. 59, no. 7, p. 1217–1232.

White, RW, Powell, R, Holland, TJB, Johnson, TE and Green, ECR 2014a, New mineral activity–composition relations for thermodynamic calculations in metapelitic systems: Journal of Metamorphic Geology, v. 32, no. 3, p. 261–286.

White, RW, Powell, R and Johnson, TE 2014b, The effect of Mn on mineral stability in metapelites revisited: New a–x relations for manganese-bearing minerals: Journal of Metamorphic Geology, doi:10.1111/jmg.12095.

Wingate, MTD, Bodorkos, S, and Kirkland, CL, 2008, 177908: quartzite, Noondeening Hill; Geochronology dataset 742, *in* Compilation of geochronology data: Geological Survey of Western Australia.

Wingate, MTD, Fielding, IOH, Lu, Y and Korhonen, FJ 2021a, 219842: granitic gneiss, Yenyening Lakes; Geochronology Record: Geological Survey of Western Australia, in prep.

Wingate, MTD, Fielding, IOH, Lu, Y, Korhonen, FJ and Quentin de Gromard, R 2021b, 208381: quartzite; Geochronology Record: Geological Survey of Western Australia,in prep.

Zibra, I 2021, Lithostructural map of the Chittering Metamorphic Belt: Geological Survey of Western Australia, digital data layer, <https://www.dmirs.wa.gov.au/geoview>.

Recommended reference

Korhonen, FJ, Blereau, ER, Kelsey, DE, Fielding, IOH and Romano, SS 2021, Metamorphic evolution of the southwest Yilgarn: Geological Survey of Western Australia, digital data layer.

Curtin University

John de Laeter Centre

The University of Western Australia

Isotope and element analyses are routinely conducted using the GeoHistory laser ablation ICP-MS and Sensitive High-Resolution Ion Microprobe (SHRIMP) ion microprobe facilities at the John de Laeter Centre (JdLC), Curtin University, with the financial support of the Australian Research Council and AuScope National Collaborative Research Infrastructure Strategy (NCRIS). The TESCAN Integrated Mineral Analyser (TIMA) instrument was funded by a grant from the Australian Research Council (LE140100150) and is operated by the JdLC with the support of the Geological Survey of Western Australia, The University of Western Australia (UWA) and Murdoch University. Mineral analyses are routinely obtained using the electron probe microanalyser (EPMA) facilities at the Centre for Microscopy, Characterisation and Analysis at UWA, and at Adelaide Microscopy, University of Adelaide.

Disclaimer

This product uses information from various sources. The Department of Mines, Industry Regulation and Safety (DMIRS) and the State cannot guarantee the accuracy, currency or completeness of the information. Neither the department nor the State of Western Australia nor any employee or agent of the department shall be responsible or liable for any loss, damage or injury arising from the use of or reliance on any information, data or advice (including incomplete, out of date, incorrect, inaccurate or misleading information, data or advice) expressed or implied in, or coming from, this publication or incorporated into it by reference, by any person whosoever.

© State of Western Australia (Department of Mines, Industry Regulation and Safety) 2021

With the exception of the Western Australian Coat of Arms and other logos, and where otherwise noted, these data are provided under a Creative Commons Attribution 4.0 International Licence. (http://creativecommons.org/licenses/by/4.0/legalcode)